IVYSPRING INTERNATIONAL PUBLISHER

Theranostics

2017; 7(7): 1806 -1819. doi: 10.7150/thno.18607

Research Paper

# Dual-pH Sensitive Charge-reversal Nanocomplex for Tumor-targeted Drug Delivery with Enhanced Anticancer Activity

Qing Zhou[1]*, Yilin Hou[2]*, Li Zhang[3], Jianlin Wang[4], Youbei Qiao[1], Songyan Guo[1], Li Fan[1], Tiehong Yang[1], Lin Zhu[5], Hong Wu[1]✉

1. Department of Pharmaceutical Analysis, School of Pharmacy, Fourth Military Medical University, Xi'an 710032, China;
2. Innovation experimental college, Northwest A&F University, Yangling 712100, China;
3. State Key Laboratory of Military Stomatology, Fourth Military Medical University, Xi'an 710032, China;
4. Department of Hepatobiliary Surgery, Xijing Hospital, Fourth Military Medical University, Xi'an 710032, China;
5. Department of Pharmaceutical Sciences, Irma Lerma Rangel College of Pharmacy, Texas A&M University Health Science Center, Kingsville, Texas 78363, United States.

* These authors contributed equally to this work.

✉ Corresponding author: Hong Wu, Department of Pharmaceutical Analysis, School of Pharmacy, Fourth Military Medical University, Xi'an 710032, China. Tel: +86-29-84776823; E-mail: wuhong@fmmu.edu.cn.



Received: 2016.12.03; Accepted: 2017.02.13; Published: 2017.04.10

## Abstract

Poly(β-L-malic acid) (PMLA), a natural aliphatic polyester, has been proven to be a promising carrier for anti-cancer drugs. In spite of excellent bio-compatibility, the application of PMLA as the drug carrier for cancer therapy is limited by its low cellular uptake efficiency. The strong negative charge of PMLA impedes its uptake by cancer cells because of the electrostatic repulsion. In this study, a dual pH-sensitive charge-reversal PMLA-based nanocomplex (PMLA-PEI-DOX-TAT@PEG-DMMA) was developed for effective tumor-targeted drug delivery, enhanced cellular uptake, and intracellular drug release. The prepared nanocomplex showed a negative surface charge at the physiological pH, which could protect the nanocomplex from the attack of plasma proteins and recognition by the reticuloendothelial system, so as to prolong its circulation time. While at the tumor extracellular pH 6.8, the DMMA was hydrolyzed, leading to the charge reversal and exposure of the TAT on the polymeric micelles, thus enhancing the cellular internalization. Then, the polymeric micelles underwent dissociation and drug release in response to the acidic pH in the lyso/endosomal compartments of the tumor cell. Both *in vitro* and *in vivo* efficacy studies indicated that the nanocomplex significantly inhibited the tumor growth while the treatment showed negligible systemic toxicity, suggesting that the developed dual pH-sensitive PMLA-based nanocomplex would be a promising drug delivery system for tumor-targeted drug delivery with enhanced anticancer activity.

Key words: PMLA, pH-sensitive, charge-reversal, TAT, cancer therapy.

## Introduction

Cancer is one of the leading causes of death around the world. According to the 2016 report of the National Center for Health Statistics, about 16.8 million new cancer cases and nearly 0.6 million of cancer deaths are projected to occur in the United States [1]. Chemotherapy is one of the most commonly used options for cancer treatment, while it may cause various undesired side effects mainly due to its low tumor targetability and off-tumor toxicity [2, 3]. Due to the unique characteristics, nanoscale drug delivery systems (NDDS) have received considerable attention in biomedical applications [4-6]. Nanoparticles of certain sizes (< 200 nm) prefer to accumulate in the tumor site through a passive targeting mechanism, *i.e.*

the enhanced permeation and retention (EPR) effect, and decrease the side effects and increase the drug's efficacy [7, 8].

In order to compose proper nanoparticles, a variety of nanomaterials have been investigated [9-11]. Due to the excellent properties, the natural or synthetic polymer-based carriers are of particular interests [12]. Among them, the PMLA emerging as a novel nanomaterial has been proved to be biodegradable, non-toxic and non-immunogenic [13, 14]. Besides, a great number of pendant carboxyl groups on PMLA provide the extra opportunities for further functionalization [14-17]. However, the strong negative charge of PMLA increases the electrostatic repulsion with the negatively charged cell membrane, leading to the low cellular uptake, and restricts its application as the drug carrier [18].

An ideal nanoparticle-based drug delivery system should possess the key characteristics, such as long circulation, high tumor accumulation and cellular uptake. PEGylation is one of the mostly used technologies to engineer the surface of the nanoparticles, to shield the undesired properties. The PEGylated nanoparticles usually have long blood circulation time due to the PEG's hindrance to the plasma proteins and the reticuloendothelial system (RES), which facilitates the EPR effect-mediated tumor targeting. However, PEGylation impedes the internalization of nanoparticles by cancer cells, and therefore is not beneficial for the cellular uptake [19-22]. In contrast, the positively charged nanoparticles effectively interact with the negatively charged cell membrane by the electrostatic attraction and trigger the efficient cell internalization [23, 24]. Nevertheless, the positive charge may cause nonspecific interactions of the nanoparticles with serum components and cell membrane of the normal cells, resulting in short circulation time and nonspecific distribution [25, 26].

Cell-penetrating peptides (CPPs), such as transactivator of transcription (TAT) peptide, were able to translocate across the cell membrane via various mechanisms. The CPP-conjugated nanoparticles have been extensively investigated as the intracellular drug delivery tools [27]. However, the lack of selectivity of CPPs may cause undesired side effects, which is one of the major obstacles and remains unresolved [28]. This dilemma is similar to that of positive surface charge of the nanoparticles. In response to these challenges, the stimuli-responsive NDDS has emerged as a smart tumor-targeted drug delivery system. Among various stimuli, pH is the most extensively exploited one for tumor-targeted drug delivery due to the pH difference between the normal tissues (pH 7.4) and tumor extracellular environment ($pH_e$ 6.8) [29, 30].

Here, a dual-pH sensitive and charge-reversal PMLA-based nanocomplex was prepared for effective drug delivery, enhanced cellular uptake, and intracellular drug release (Fig. 1). The PMLA was first modified with polyethylenimine (PEI) to allow the polymer to bear the positive charge (PMLA-PEI). Covalent conjugation of pH-sensitive *cis*-aconitic anhydride-modified doxorubicin (DOX-CA) with PMLA afforded the amphiphilic co-polymers that readily formed the polymeric micelles by the dialysis method (PMLA-PEI-DOX). The TAT peptide was conjugated to the PMLA (PMLA-PEI-DOX-TAT) to further increase the cellular uptake efficiency of polymeric micelles. Then, the 6-armed polyethylene glycol (PEG) decorated with 2,3-dimethylmaleic anhydride (DMMA) (PEG-DMMA), was used to 'wrap'/modify the polymeric micelles, to shield the positive charge and TAT peptide. The obtained dual pH-sensitive charge-reversal nanocomplex (PMLA-PEI-DOX-TAT@ PEG-DMMA) was a 'Trojan horse'-like system. In the blood (at normal pH), the PEGylated nanocomplex is negatively charged, which prolongs its circulation time and minimizes the rapid clearance of the nanocomplex from the body. However, the nanocomplex undergoes the PEG deshielding via the pH-sensitive hydrolysis of DMMA in the tumor microenvironment, leading to a quick conversion from the negative charge to the positive charge. The resultant positively charged and TAT exposed polymeric micelles would be efficiently internalized by the tumor cells. After endocytosis, the polymeric micelles could rapidly release the loaded drugs at the endosomal/lysosomal pH, to facilitate the drug action. All these make this dual-pH sensitive charge-reversal nanocomplex as a smart drug nanocarrier with enhanced tumor inhibition efficacy.

## Results and Discussion

### Synthesis and characterization of polymers

The entire synthetic routes for PMLA-PEI-DOX-TAT, PEG-DMMA and PEG-SA are illustrated in Fig. S1. Firstly, PMLA was modified by PEI, and the degree of substitution (DS) of PEI over PMLA was 0.4%. Then pH-sensitive doxorubicin prodrug (DOX-CA) was synthesized through the reaction between doxorubicin and *cis*-aconitic anhydride. After that, DOX-CA reacted with 1,4-diaminobutane to provide amino groups for the conjugation with PMLA, thus polymer PMLA-PEI-DOX was obtained. In order to conjugate TAT to the polymer, TAT-cysteine peptide firstly reacted with N-(2-aminoethyl)maleimide through maleimide-thiol covalent coupling, and since N-(2-aminoethyl)

maleimide could provide the amino groups, then the polymer PMLA-PEI-DOX-TAT was obtained by the reaction between the amino groups and carboxyl groups in PMLA. The obtained PMLA-PEI-DOX-TAT was identified by $^1$H NMR. As shown in Fig. S2, the signals at 2.95 and 5.38 ppm were assigned to methylene and methane protons of PMLA respectively. The signals at 2.13-2.33 ppm were assigned to the protons of -NHCH$_2$CH$_2$- of PEI. The signals at 3.99, 4.58 and 7.93 ppm were assigned to the benzene, methyl and methane protons of DOX respectively. The $^1$H-NMR spectra indicated the successful synthesis of polymer PMLA-PEI-DOX-TAT.

Due to extreme sensitivity to tumor pH$_e$, DMMA was used to design pH-sensitive deshielding PEG layer [31-33]. Non charge-reversal SA-conjugated PEG was chosen as a control. DMMA or SA was conjugated to 6NH$_2$-PEG through the reaction between the amines in 6NH$_2$-PEG and the anhydride in DMMA or SA, and the resultant PEG-DMMA and PEG-SA were also identified by $^1$H NMR. The signals at 3.09-3.84 ppm were assigned to methylene protons of PEG. While the signal at 1.97 ppm represented the methyl of DMMA, the signals of methyl of SA appeared at 2.49 and 2.46 ppm after the conjugation (Fig. S3 and S4). The $^1$H-NMR spectra indicated the successful synthesis of PEG-DMMA and PEG-SA. According to UV-vis absorbance at 481 nm, the DOX content in the polymer-drug conjugates was 17.71 wt.% for PMLA-PEI-DOX and 16.82 wt.% for PMLA-PEI-DOX-TAT (Table S1).

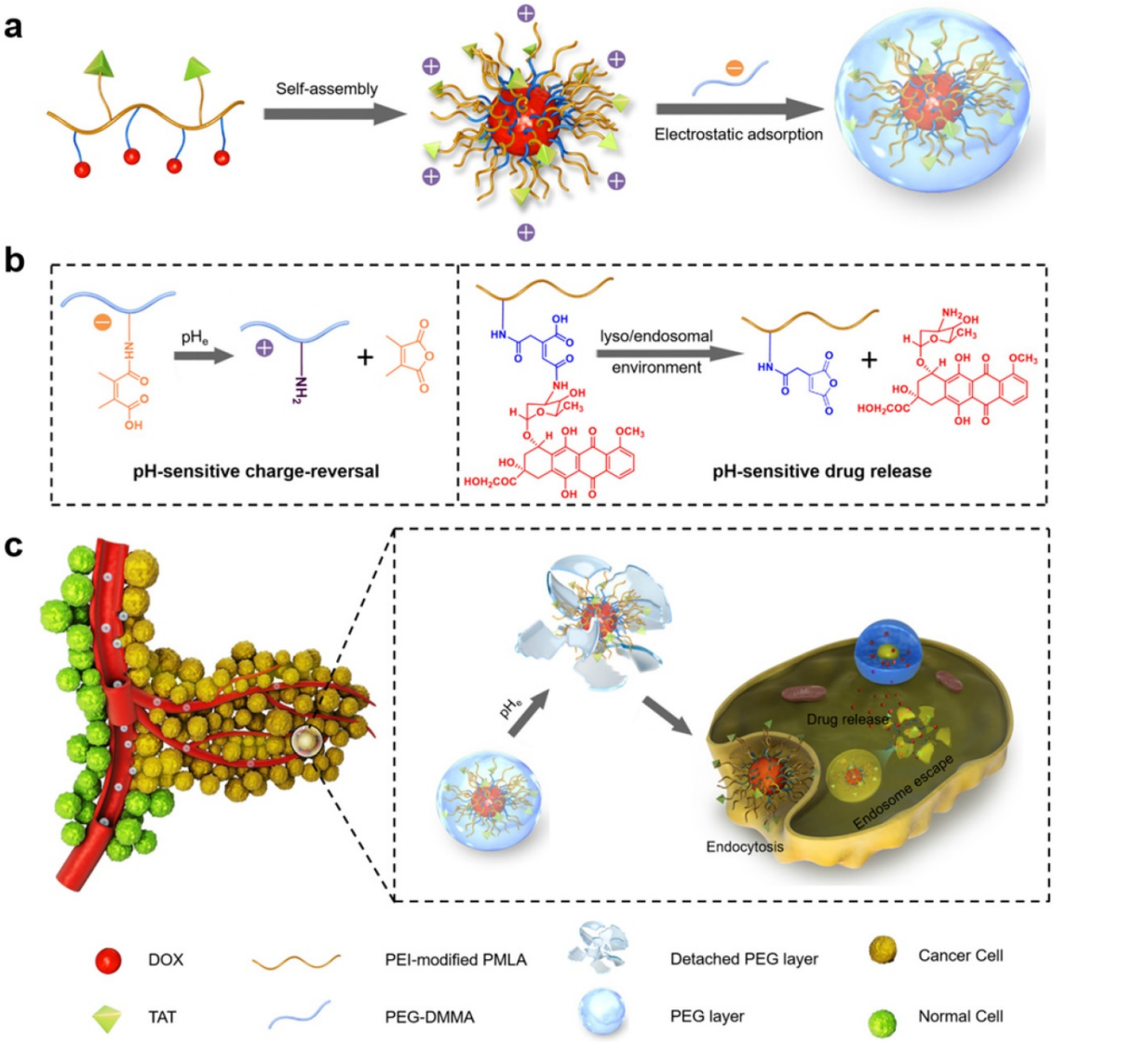


**Figure 1.** (a) Preparation of nanocomplex PMLA-PEI-DOX-TAT@PEG-DMMA. (b) Illustration of the dual pH-sensitive property, pH-sensitive charge-reversal and pH-sensitive drug release. (c) Schematic illustration of the dual pH-sensitive DOX-loading nanocomplex with the charge-conversional function for effective tumor-targeted drug delivery, enhanced cellular uptake, and intracellular drug release.

### Preparation and characterization of polymeric micelles and nanocomplexes

The polymeric micelles were then constructed from the PMLA-PEI-DOX-TAT via self-assembly, followed by shielding with the pH-sensitive charge-reversal PEG-DMMA or non-charge-reversal PEG-SA through electrostatic adsorption. The four types of the polymeric micelles (PMLA-PEI-DOX and PMLA-PEI-DOX-TAT) or nanocomplexes (PMLA-PEI-DOX-TAT@PEG-SA and PMLA-PEI-DOX-TAT@PEG-DMMA) were prepared. In our previous study, the charge-conversional nanoconjugates based on PMLA were prepared for effective and specific anti-tumor drug delivery [18]. Compared to the nanoconjugates, the nanocomplex was more stable and convenient, more importantly, possessed the stimuli-responsive properties, the pH-sensitive charge reversal and pH-sensitive drug release.

The dynamic light scattering (DLS) measurement showed that the average particle size of the DOX-loaded nanoparticles was 108.3 ± 5.5 nm for PMLA-PEI-DOX, 95.0 ± 5.7 nm for PMLA-PEI-DOX-TAT, 126.1 ± 3.5 nm for PMLA-PEI-DOX-TAT@PEG-SA, and 123.0 ± 2.2 nm for PMLA-PEI-DOX-TAT@PEG-DMMA, respectively (Fig. 2a, Fig. S5 and Table S1). Based on the TEM image, the PMLA-PEI-DOX-TAT@PEG-DMMA showed a spherical morphology with a size of 100.6 ± 3.1 nm that was smaller than DLS measurement due to the hydrodynamic radius in the aqueous buffer (Fig. 2a). The zeta potential of these micelles were +10.47 ± 0.51 mV, +23.51 ± 0.76 mV, -16.04 ± 0.34 mV and -16.33 ± 0.63 mV, respectively. The CMC value of PMLA-PEI-DOX-TAT was 5.222 mg/L, which was determined by fluorescent spectroscopy using pyrene as a probe (Fig. S5d). These results indicated that DOX-conjugated polymers were successfully self-assembled into the core-shell structured micelles in aqueous solution, in which DOX molecules were packed in the core through hydrophobic interaction, while PMLA-PEI acted as the shell. Moreover, the nanocomplex PMLA-PEI-DOX-TAT@PEG-DMMA exhibited excellent stability in different physiological solutions, including PBS (pH 7.4) and RPMI 1640 medium with 10% FBS (Fig. S6b).

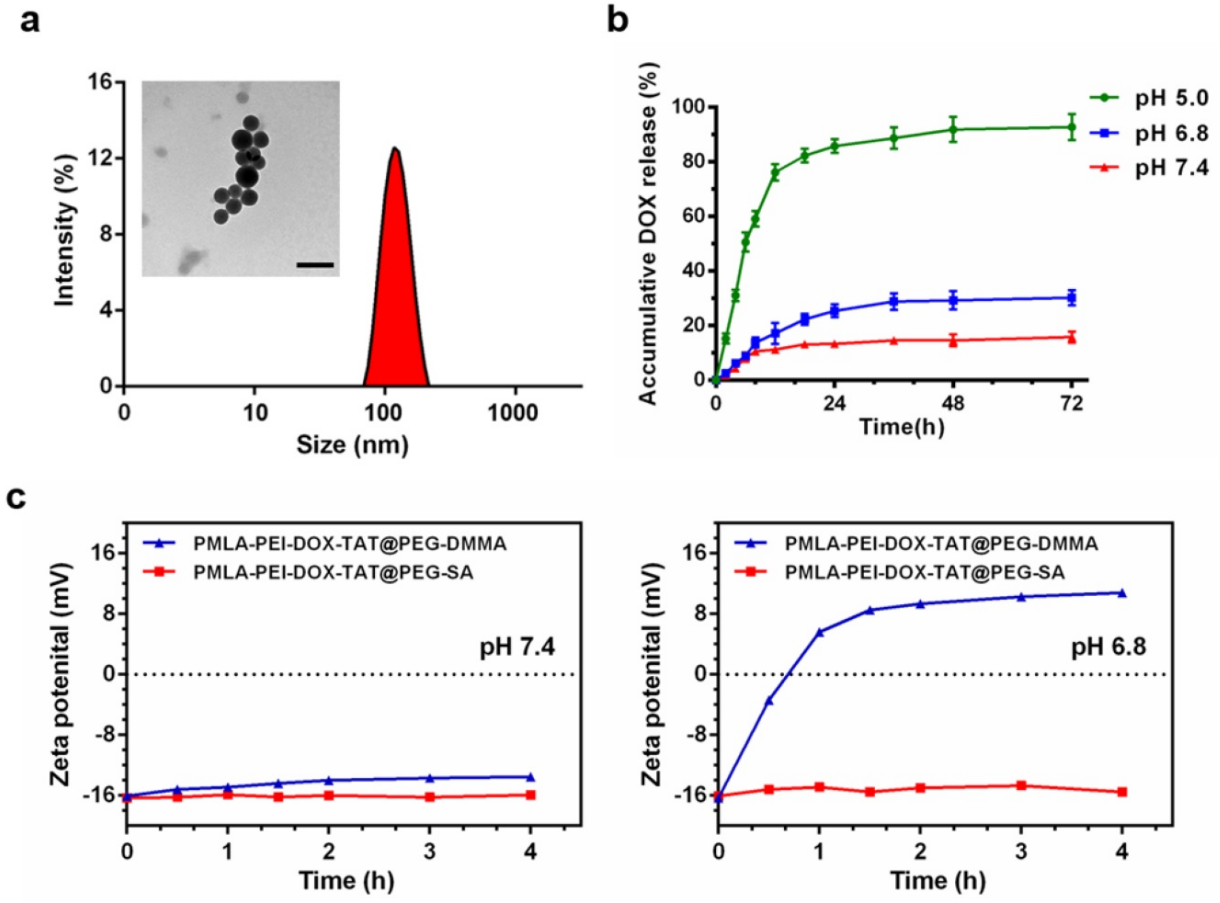


**Figure 2.** (a) DLS and TEM results of the nanocomplex PMLA-PEI-DOX-TAT@PEG-DMMA, the scale bar is 200 nm. (b) Release profile of DOX from the nanocomplex PMLA-PEI-DOX-TAT@PEG-DMMA in PBS (pH 5.0, pH 6.8 or pH 7.4) at 37 °C. (c) Zeta potential changes of PMLA-PEI-DOX-TAT@PEG-DMMA and PMLA-PEI-DOX-TAT@PEG-SA nanocomplexes when incubating at pH 7.4 and 6.8 for different time periods.

In our previous study, DOX was directly conjugated to PMLA via the amide bond and the formed nanoconjugates showed a pH-sensitive drug release pattern [18]. Nevertheless, it's uncertain whether the released drug formulation was free DOX or not, the pH-sensitive pattern probably caused by the hydrolysis of PMLA at acid environment. Thus, in this work, DOX was conjugated to PMLA-PEI via a pH-sensitive maleic acid amide bond and ensured effective release of free DOX in response to the acidic endosomal/lysosomal pH. As shown in Fig. S7, free DOX exhibited its peak at an elution time of 2.82 min and DOX-CA exhibited its peak at an elution time at 1.15 min. Furthermore, the incubation of DOX-CA at pH 4.0 and pH 5.0 resulted in significant degradation, with a half-life of 3.5 h and 1 h respectively (Fig. S7b). The intensity of the peaks DOX-CA decreased while the intensity of the peaks of free DOX increased sharply at pH 5.0 and pH 4.0. In contrast, no degradation was observed and the maleic acid amide bonds in DOX-CA were very stable under pH 7.4 and pH 6.8 at 37 °C for 12 h. In addition, the incubation of PMLA-PEI-DOX-TAT at acidic environment revealed that the released drug formulation from the polymer was free DOX (Fig. S7c). These results indicated that the maleic acid amide bonds in DOX-CA could be cleaved under endo/lysosomes conditions of cancer cells, resulting in the release of free DOX, while remain stable under normal physiological conditions and in extracellular environment.

Release of DOX from the nanocomplex PMLA-PEI-DOX-TAT@PEG-DMMA was also measured in order to confirm the pH sensitivity of the nanocomplex. The *in vitro* DOX release profile of the nanocomplex was investigated at different pH values (Fig. 2b). The nanocomplex exhibited the relatively high stability at pH 7.4 with a no more than 20% DOX release after 72 h, while the drug release rate slightly increased at pH 6.8, which was caused by the hydrolysis of the DMMA. However, when the pH declined to 5, a rapid drug release was observed. The DOX release at pH 5.0 was in a biphasic manner, an initial rapid release in 12 h followed by a slow and continuous release for up to 72 h, and the cumulative release of DOX from the nanocomplex was over 90% after 3 days. This result was due to the quick cleavage of the acid-sensitive amide bond between DOX and PMLA at lower pH (the endosomal and lysosomal environments). This suggested that the nanocomplex PMLA-PEI-DOX-TAT@PEG-DMMA might hold the drugs under physiological condition and reduce the *in vivo* drug leakage, and release the drug in response to the endosomal pH (pH 5~6) or lysosomal pH (pH 4~5), to ensure the drug action in the intracellular compartment, i.e. cell nuclei.

DMMA was extremely sensitive to acidic tumor extracellular microenvironment ($pH_e$, ~6.8), the negatively charged polymer PEG-DMMA could be hydrolyzed to become positively charged $6NH_2$-PEG, and then the PEG layer could detach from the positively charged PMLA-PEI-DOX-TAT due to the electrostatic repulsion. This property was confirmed by the zeta potential of PMLA-PEI-DOX-TAT@PEG-DMMA at the tumor extracellular pH 6.8 and normal physiological pH 7.4 (Fig. 2c). PMLA-PEI-DOX-TAT@PEG-SA was chosen as a control, because PEG-SA was stable under the acidity of the tumor. At pH 7.4, both PMLA-PEI-DOX-TAT@PEG-DMMA and PMLA-PEI-DOX-TAT@PEG-SA exhibited non-charge reversal characteristics with a consistent negative charge after incubation at 37 °C for 4 h, while at pH 6.8, PMLA-PEI-DOX-TAT@PEG-DMMA showed obvious charge-reversal property from the negative charge to positive charge (from -16.33 to +10.81 mV) after incubation at 37 °C for 4 h, and PMLA-PEI-DOX-TAT@PEG-SA did not exhibit the charge conversion.

It is believed that most of amide bonds only can be degraded at extreme pH values (pH < 1 or pH > 13), while maleic acid amide derivatives can be degraded at mild acidic pH values [34, 35]. In this study, we used two maleic acid amide derivatives, *cis*-aconitic acid amide and dimethylmaleamidic acid amide, to obtain pH-sensitive degradability, one for pH-sensitive drug release and the other one for pH-sensitive charge-reversal. *cis*-aconitic acid amide was used as pH-sensitive linker between DOX and PMLA since it contains two carboxylate groups, the β-carboxylate group for pH degradability to release free DOX and the other group for linking with PMLA. Dimethylmaleamidic acid amide was employed to design acidity-controlled charge-reversal deshielding systems due to its extreme sensitivity to tumor $pH_e$. The difference of pH-sensitivity between two maleic acid amide derivatives was caused by the difference of their chemical structure, particularly the substituents of the *cis*-double bonds. *cis*-aconitic acid amide with one carboxyethyl and one hydrogen substituent showed appropriate degradability at the endosomal/lysosomal pH, while two methyl groups substituent on dimethylmaleamidic acid amide played a crucial role in the extreme pH-sensitivity ($pH_e$).

## Cellular Uptake Measured by Confocal Laser Scanning Microscopy (CLSM) and Flow Cytometry

Confocal laser scanning microscopy (CLSM) analysis and flow cytometry study were performed to investigate the effects of the pH-sensitive

charge-reversal property on the cellular uptake of nanoparticles. The Cy3-labeled polymeric micelles (PMLA-PEI-DOX and PMLA-PEI-DOX-TAT) or nanocomplexes (PMLA-PEI-DOX-TAT@PEG-SA and PMLA-PEI-DOX-TAT@PEG-DMMA) were incubated with cancer cells for 4 hours at pH 7.4 or 6.8.

As shown in Fig. 3, in A549 cells, the PMLA-PEI-DOX-TAT group showed the strongest intracellular fluorescence of Cy3 at both pH 7.4 and 6.8, indicating the combination of positive charge and TAT could greatly enhance the cellular uptake. Compared with PMLA-PEI-DOX-TAT group, the PMLA-PEI-DOX group showed much lower intracellular fluorescence, suggesting that TAT was more efficient to induce the endocytosis than the PEI. At pH 7.4, both nanocomplexes (PMLA-PEI-DOX-TAT@PEG-SA and PMLA-PEI-DOX-TAT@PEG-DMMA) showed low intracellular fluorescence. The electrostatic repulsion between the negatively charged nanoparticles and cell membranes decreased the cell uptake. However, when the pH declined to 6.8, due to the exposure of positively charged TAT-conjugated polymeric micelles, the PMLA-PEI-DOX-TAT@PEG-DMMA group showed much higher intracellular fluorescence. In contrast, the intracellular fluorescence of PMLA-PEI-DOX-TAT@PEG-SA group was similar to that at pH 7.4. As shown in Fig. 4, at pH 7.4, the cellular uptake of the PMLA-PEI-DOX-TAT@PEG-SA and PMLA-PEI-DOX-TAT@PEG-DMMA was almost identical. PMLA-PEI-DOX showed a little bit higher cellular uptake due to the positive charge surface, and the uptake of PMLA-PEI-DOX-TAT was the highest. While at pH 6.8, the cellular uptake of PMLA-PEI-DOX-TAT@PEG-DMMA was greatly enhanced. All these results were consistent with CLSM analysis.

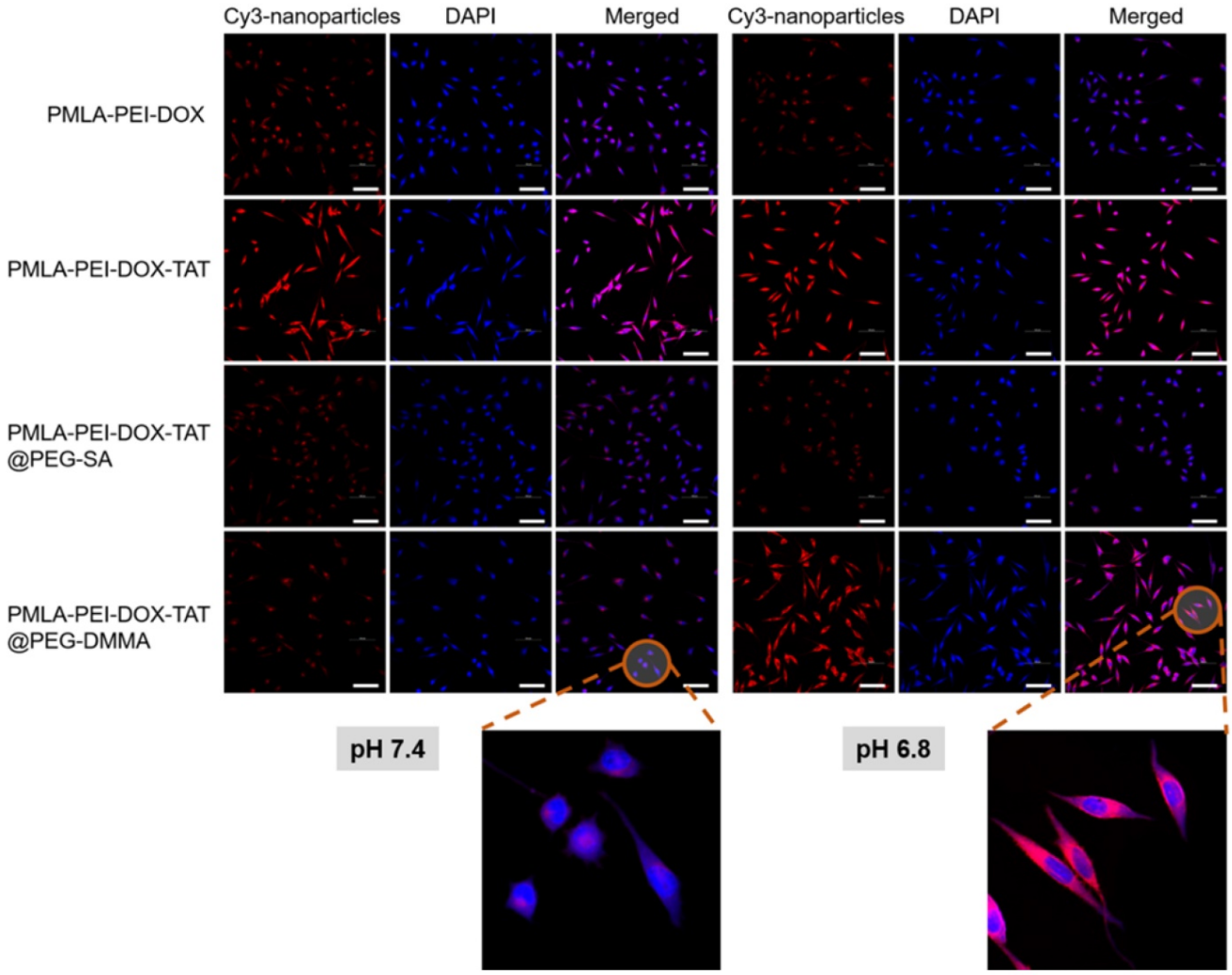


**Figure 3.** Confocal microscopic images of cellular internalization of Cy3-labeled nanoparticles by A549 cells incubated at pH 7.4 and 6.8 for 4 h. DAPI (blue) was used to stain cell nucleus. The scale bar is 100 μm.

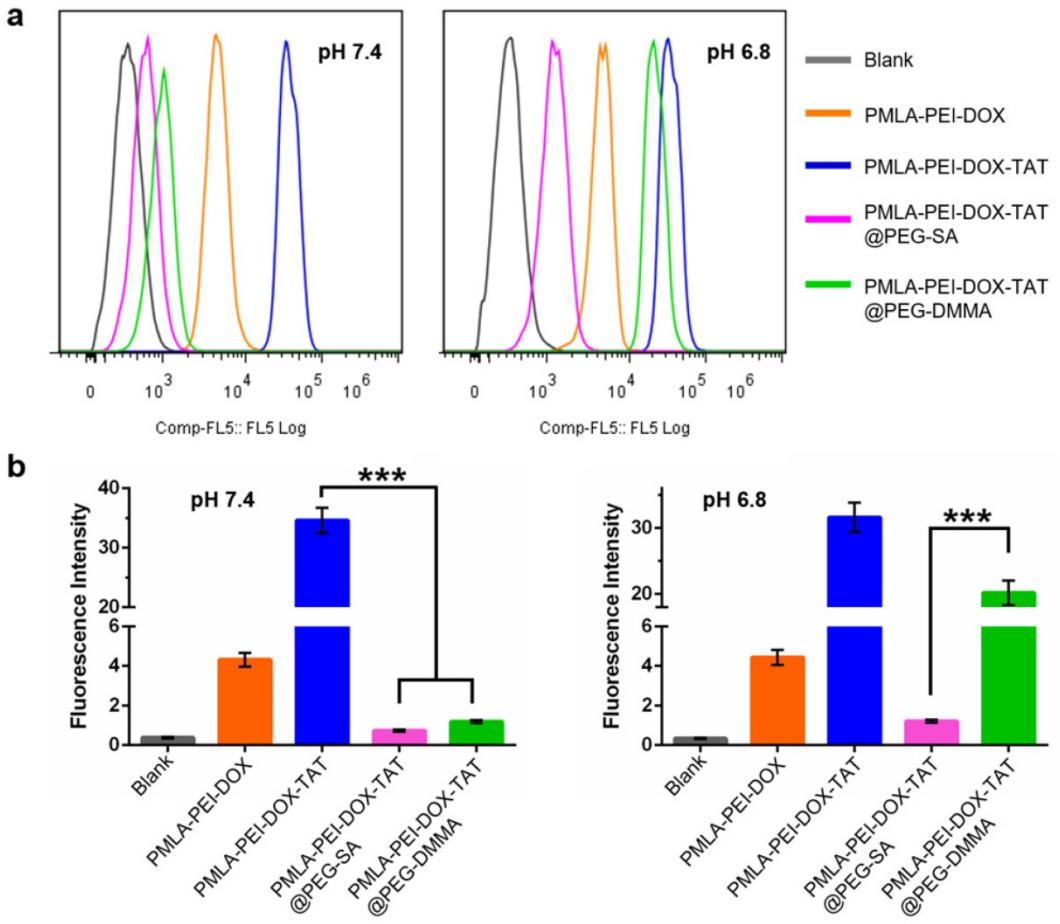


**Figure 4.** (a) Flow cytometry analysis of cellular uptake of Cy3-labeled nanoparticles by A549 cells at pH 7.4 and pH 6.8 conditions for 4 h. (b) Quantitative analysis of the fluorescence intensity of Cy3-labeled nanoparticles in A549 cells.

To further confirm the cellular uptake results, in addition to the lung cancer cells A549, human hepatocellular carcinoma cells MHCC97-H were also used as the *in vitro* cancer models. In MHCC97-H cells, the PMLA-PEI-DOX-TAT group showed the highest cellular uptake at both pH 7.4 and 6.8 (Fig. S9 and S10), which was consistent with the results in the A549 cells. In addition, the nanocomplexes PMLA-PEI-DOX-TAT@PEG-SA and PMLA-PEI-DOX-TAT@PEG-DMMA displayed comparable intracellular fluorescence at pH 7.4, while the cellular uptake of the positively charged polymeric micelles PMLA-PEI-DOX was about 4-fold increased (Fig. S10), indicating that the positive charge could facilitate the interaction with negatively charged cell membrane to promote the cellular internalization. However, when the pH decreased from 7.4 to 6.8, the hydrolysis of DMMA caused the charge reversal of PEG layer, resulting in the exposure of the positively charged TAT-conjugated polymeric micelles (PMLA-PEI-DOX-TAT), so as to enhance the cell internalization. All these results indicate that the combination of the positive charge and TAT could greatly promote the cellular uptake of the nanoparticles and the cellular uptake of the nancomplex, PMLA-PEI-DOX-TAT@PEG-DMMA, was pH-dependent.

### *In Vitro* Cytotoxicity Study

*In vitro* antitumor activities of various DOX formulations were evaluated by Cell Counting Kit-8 (CCK-8) assay on A549 and MHCC97-H cells, and 50% inhibitory concentration ($IC_{50}$) was determined. In A549 cells, as shown in Fig. 5 and Table S2, the pH value of the culturing media hardly affected the cytotoxicity of the free DOX, PMLA-PEI-DOX, PMLA-PEI-DOX-TAT and PMLA-PEI-DOX-TAT@PEG-SA. The PMLA-PEI-DOX-TAT@PEG-DMMA showed the comparable cytotoxicity with the PMLA-PEI-DOX-TAT@PEG-SA at pH 7.4, but had an 8.97-fold lower $IC_{50}$ value at pH 6.8. Higher cytotoxicity was probably caused by higher cellular uptake. At both pH 7.4 and 6.8, the PMLA-PEI-DOX-TAT showed the lowest $IC_{50}$ value, indicating the great cellular uptake efficacy caused by the combinatory effects of the positive charge and TAT. In MHCC97-H cells, at pH 7.4, no statistical difference was observed between the PMLA-

PEI-DOX-TAT@PEG-SA and PMLA-PEI-DOX-TAT@PEG-DMMA (Fig. S11 and Table S3). However, the cell death increased significantly when the cancer cells were incubated with PMLA-PEI-DOX-TAT@PEG-DMMA at pH 6.8 due to the charge-reversal induced cellular internalization.

The cytotoxicity profiles of various DOX formulations indicated that the combination of the positive charge and TAT in the nanoparticles would have a synergistic effect on cytotoxicity. Besides, the cytotoxicity of polymers (PMLA-PEI, PMLA-PEI-TAT, PEG-DMMA and PEG-SA) without DOX conjugation was also evaluated. As shown in Fig. S11c, the polymers without DOX conjugation exhibited negligible cytotoxicity against A549 cells at various concentrations ranged from 0.1 to 1000 μg/mL for 48 h at pH 7.4, which indicated that the polymers were biocompatible and safe.

### *In Vivo* Tumor growth Inhibition Study

The antitumor activity of the nanocomplex, PMLA-PEI-DOX-TAT@PEG-DMMA, and other DOX formulation were measured in A549 xenograft mouse model. Firstly, in order to demonstrate the targeting effect of the nanoparticles, the bio-imaging study was conducted using an *in vivo* fluorescence imaging system. Fluorescent images of the treated mice were recorded at 24 h post injection using an IVIS® Spectrum Imaging System. As shown in Fig. 6, mice treated with Cy3-labled nanocomplexes, PMLA-PEI-DOX-TAT@PEG-SA and PMLA-PEI-DOX-TAT@PEG-DMMA, showed strong fluorescence signal at the tumor site, indicating a better tumor targeting efficiency. In contrast, almost no fluorescence was detected in the tumor after 24 h of treatment with Cy3-labled polymeric micelles PMLA-PEI-DOX and PMLA-PEI-DOX-TAT. The relatively stronger fluorescence was observed mainly in the liver and kidney, indicating that the positively charged nanoparticles, PMLA-PEI-DOX and PMLA-PEI-DOX-TAT, would be more likely to be captured by the liver and kidney rather than the tumor. Although the mice treated with the negatively charged and PEG-coated nanocomplexes showed some fluorescence in the liver and kidney, the fluorescence is remarkably low compared to the positively charged polymeric micelles. All these results suggest that the negative surface charge and PEG coating could reduce the nonspecific protein binding, avoid the opsonization by RES, and facilitate the ERP effect-mediated tumor accumulation.

As shown in Fig. 7a, the tumor volume of the saline-treated group rapidly increased over 21 days. The PMLA-PEI-DOX-TAT and PMLA-PEI-DOX@PEG-SA moderately inhibited tumor growth. In contrast, the PMLA-PEI-DOX@PEG-DMMA displayed the highest tumor inhibition effect. The growth of tumors on free DOX injected mice was slightly inhibited over 9 days. Moreover, we also measured the weight of each tumor mass at the end of the treatment (Fig. 7c), which confirmed that the tumor growth inhibition data. In addition, the H&E and TUNEL examination of tumor sections (Fig. 7d) showed that the PMLA-PEI-DOX-TAT@PEG-DMMA treated group resulted in significantly reduced proliferation and increased apoptosis compared that of the other groups.

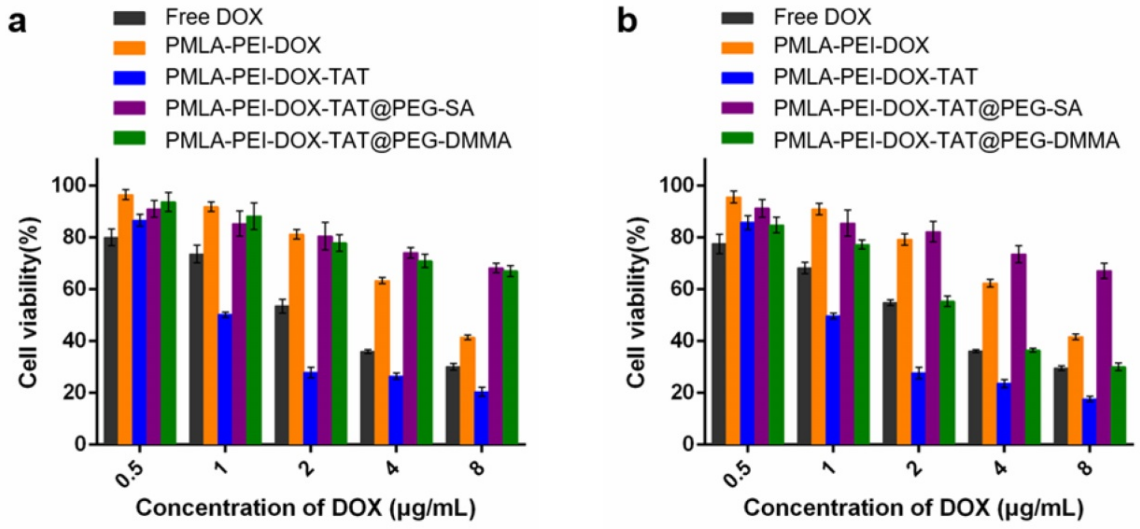


**Figure 5.** Cytotoxicity of Free DOX and various nanoparticles against A549 cells at different concentrations of DOX under (a) pH 7.4 and (b) pH 6.8 for 48 h.

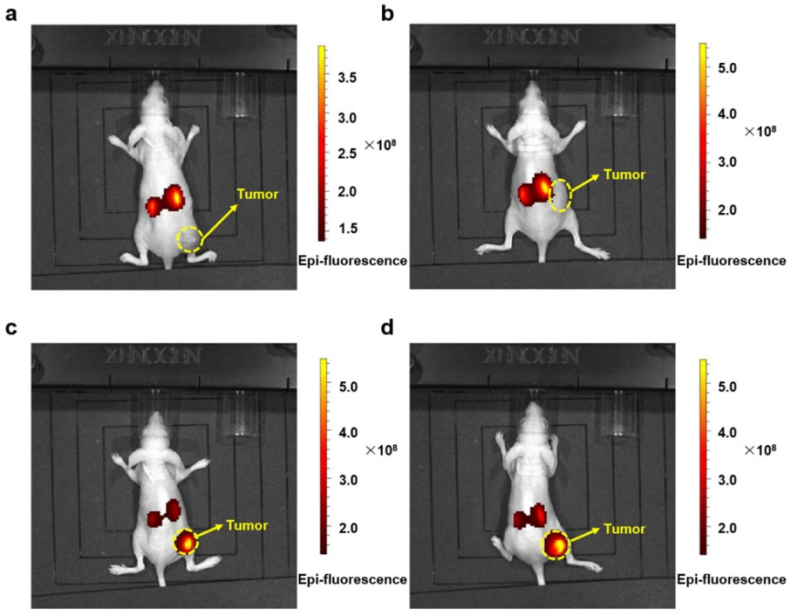


**Figure 6.** *In vivo* imaging of tumor bearing mice. Fluorescent signal captured by IVIS Lumina Imaging System in tumor bearing mice after injection with Cy3-labeled PMLA-PEI-DOX (a), PMLA-PEI-DOX-TAT (b), PMLA-PEI-DOX-TAT@PEG-SA (c) and PMLA-PEI-DOX-TAT@PEG-DMMA (d) for 24 h.

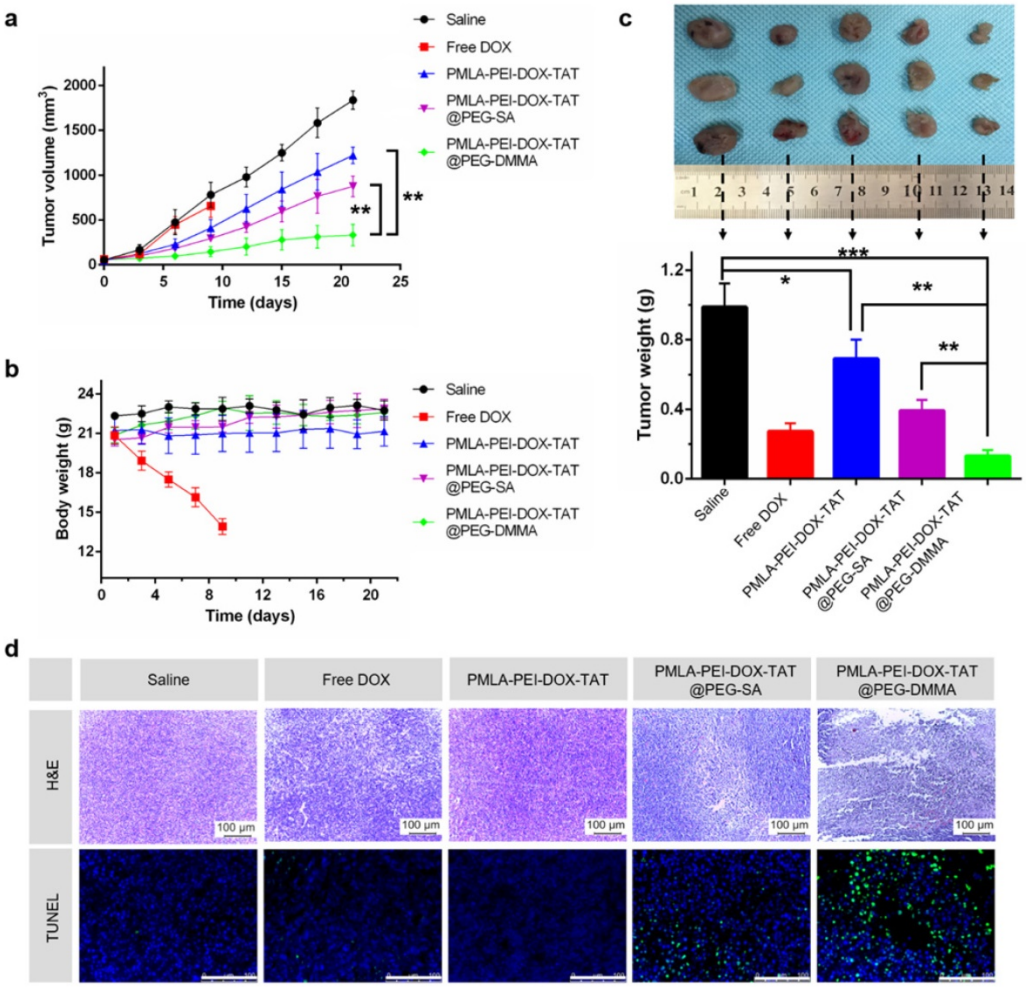


**Figure 7.** The antitumor effect of nanocomplex on nude mice bearing A549 cells subcutaneously. (a) The variation profiles of tumor volumes during injection. (b) The variation profiles of body weights during injection. (c) Dissected tumor tissues from the nude mice (Free DOX group, survived for 9 days and the weight of dissected tumor tissues. (d) H&E and TUNEL examination of the tumors from mice bearing A549 mammary tumors after 21-day injection. Data was given as mean ± SD (n=4). The scale bar is 100 μm.

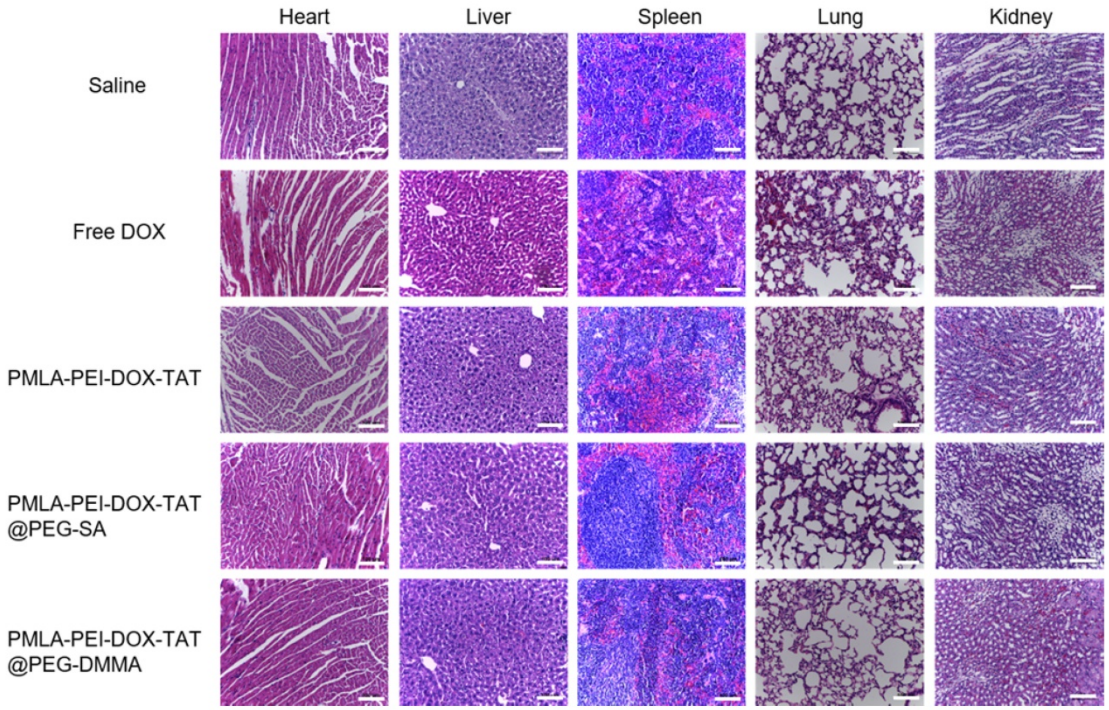


**Figure 8.** Histopathological analysis. Images of tissue sections stained with Hematoxylin and Eosin after treatments with Saline, Free DOX, PMLA-PEI-DOX-TAT, PMLA-PEI-DOX-TAT@PEG-SA and PMLA-PEI-DOX-TAT@PEG-DMMA. The scale bar is 100 μm.

Body weight changes in all mice groups, as an indicator of systemic toxicity, were measured (Fig.7b). Serious systemic toxicity was observed in animals treated with free DOX ($p$<0.05). The death of mice was observed on the 9th after free DOX treatment. However, the body weight of other four groups was not obviously affected over the investigation period, indicating that the nanoparticles could reduce the side effect of drugs. In addition, the histological analysis of the main organs including heart, liver, spleen, lung, and kidney was shown in Fig. 8. There were no apparent damages in the detected organs from free DOX group, PMLA-PEI-DOX-TAT group, PMLA-PEI-DOX-TAT@PEG-SA group, PMLA-PEI-DOX-TAT@PEG-DMMA group, and control group. The results demonstrate that the nanocomplex PMLA-PEI-DOX-TAT@PEG-DMMA could improve the drug's anticancer activity and decrease its side effects.

## Conclusion

In summary, a dual pH-sensitive charge-reversal nanocomplex PMLA-PEI-DOX-TAT@PEG-DMMA was successfully prepared for effective drug delivery, enhanced cellular uptake and intracellular drug release. At normal physiological condition (pH 7.4), the nanocomplex showed a negative surface charge. While at tumor extracellular microenvironment ($pH_e$ 6.8), the pH-sensitive charge-reversal PEG-DMMA layer would be taken off, resulting in the exposure of the positively charged TAT-conjugated polymeric micelles, so as to enhance cell internalization. After internalization, the polymeric micelles could facilitate the escape from endosome/lysosome of tumor cells, simultaneously trigger the drug release, and ensure the nuclear delivery of the anticancer drug. The nanocomplex showed high tumor accumulation and excellent tumor growth inhibition in both the cancer cells and xenograft. The study indicated that the nanocomplex, PMLA-PEI-DOX-TAT@PEG-DMMA, could be a promising nanocarrier for tumor-targeted drug delivery with enhanced anticancer activity.

## Materials and Methods

### Materials

TAT-cysteine peptide (TATp-Cys 12-mer: CysTyrGlyArgLysLysArgArgGlnArgArgArg; molecular mass 1662.99 Da with one reactive thiol group) was synthesized by KE BIOCHEM company (Shanghai, China). Polyethyleneimine (PEI with a MW of 1.8 kDa, branched) and Doxorubicin hydrochloride (DOX•HCl) were purchased from Sigma-Aldrich (Shanghai, China). 2,3-dimethylmaleic anhydride (DMMA), succinic anhydride (SA) and *cis*-aconitic anhydride (CA) were purchased from Alfa Aesar (Beijing, China). N-(2-aminoethyl)maleimide trifluoroacetic acid was purchased from Energy Chemical (Shanghai, China). 1-(3-dimethylaminopropyl)-3-ethylcarbodiimide hydrochloride (EDC•HCl) an

d N-hydroxysuccinimide (NHS) were purchased from TCI (Shanghai, China). 1,4-diaminobutane and N-(2-aminoethyl)maleimide trifluoroacetic acid were purchased from J&K SCIENTIFIC LTD (Shanghai, China). 6-armed polyethylene glycol (PEG) (Mw: 10 kDa) was purchased from Sunbio (Korea). Cy3-PEG2000-$NH_2$ was purchased from Nanocs Inc. (New York, USA). HPLC-grade acetonitrile and methanol were purchased from Merck (Darmstadt, Germany). All solvents were thoroughly dried and distilled before use. RPMI-1640 medium, Dulbecco's modified Eagle's medium (DMEM) and fetal bovine serum (FBS) were purchased from Hyclone Cell Culture and Bioprocessing (Thermo Scientific, USA). EnoGeneCell™ Counting Kit–8 (CCK-8) and 4',6-diamidino-2-phenylindole (DAPI) were purchased from Beyotime Institute of Biotechnology (Shanghai, China).

## Synthesis of polymers

PMLA (Mw: 7.89 kDa) was synthesized by ring-opening polymerization and then modified with PEI to obtain positive charge as described in our previous study [18]. DOX-CA was synthesized by the ring-opening reaction between DOX and CA with triethylamine (TEA) as catalyst. In DMF (10 mL), DOX▪HCl (58 mg), CA (17.2 mg) and triethylamine (8.4 μL) were added. After reacting at room temperature under nitrogen atmosphere for 24 h, the mixture was added EDC▪HCl (40 mg) and NHS (25 mg) for another 4 h reaction. Then, the mixture was dropwise added into1,4-diaminobutane (0.11 mmol, 9.8 mg) solution for 12 h reaction in dark. After that, pH-sensitive DOX-CA was conjugated to PMLA-PEI via amide reaction, thus polymer PMLA-PEI-DOX was obtained. TAT-cysteine peptide (0.003mmol, 5 mg) and N-(2-aminoethyl)maleimide (0.003mmol, 0.765 mg) were dissolved in 4 mL DMSO, then the solution was stirred at room temperature for 12 h. Subsequently, the solution was added into the solution of polymer PMLA-PEI-DOX for 12 h reaction to obtain polymer PMLA-PEI-DOX-TAT. Finally, the mixture was dialyzed against water for 48 h by using a dialysis membrane with MWCO of 12 kDa. After being frozen dried, the obtained polymer PMLA-PEI-DOX-TAT was stored at −20 °C for further use. In addition, Cy3-labled polymers were synthesized by the reaction between the amino groups in Cy3-PEG-$NH_2$ and carboxyl groups in PMLA.

## Synthesis of PEG-DMMA and PEG-SA

In ~ pH 8.5 PBS (20 ml), 6$NH_2$-PEG (50 mg, 10 kDa) was dissolved. Then, DMMA (152 mg) or SA (127 mg) was added slowly into the solution. After reacting at room temperature for 24 h, the mixture was dialyzed against water for 48 h by using a dialysis membrane with MWCO of 8 kDa. After being frozen dried, the obtained polymer PEG-DMMA or PEG-SA were stored at −20 °C for further use.

## Characterization of polymers

The synthesized polymers PMLA-PEI-DOX-TAT, PEG-DMMA and PEG-SA were confirmed by $^1$H NMR. NMR spectra were obtained by Varian 400 MHz (Bruker, Germany). Chemical shifts were expressed as parts per million (ppm). UV-Vis spectroscopy (Shimadzu, Japan) was used to quantify the amount of DOX conjugated on the polymers. Briefly, DOX-conjugated polymers were dissolved in deionized water and the absorbance of the solutions at 481 nm was measured. Using a calibration curve obtained by measuring the absorbance of different concentrations of free DOX in deionized water at 481 nm, and the DOX content in the polymer was calculated. The critical micelle concentration (CMC) of polymer was determined with fluorescent spectroscopy using pyrene as a probe. Polymer solution with a series of concentration range from $8\times10^{-4}$ to 0.8 mg/mL and a solution of pyrene in acetone ($1\times10^{-5}$ mol/L) were prepared. Then, 1 mL pyrene solution was taken, after evaporation of the solvent, 10 mL polymer solution was added. The excitation wavelength was set at 335nm and the measured emission wavelengths were set at 373 and 383 nm.

## Preparation and characterization of the polymeric micelles and nanocomplexes

The PMLA-PEI-DOX-TAT micelle was prepared as described below: PMLA-PEI-DOX-TAT (80 mg) was dissolved in DMSO (2 mL), and the solution in DMSO was added dropwise to the water under stirring. The mixed solution was dialyzed in 10 kDa dialysis bag with the water changing every 2 h for 24 h. Then polymeric micelles PMLA-PEI-DOX-TAT complexed with PEG-DMMA or PEG-SA was proceeded. PMLA-PEI-DOX-TAT (1.0 mL, 1 mg/mL in water) was added dropwise to PEG-DMMA or PEG-SA (2.0 mL, 1 mg/mL in water), respectively. The solution was stirred at room temperature overnight before being frozen dried, and the obtained EG-DMMA or PEG-SA complexed PMLA-PEI-DOX-TAT@PEG-DMMA or PMLA-PEI-DOX-TAT@PEG-SA was stored at −20 °C for further use. The particle size of polymeric micelles and nanocomplexes were measured by Delsa™ Nano C Particle Analyzer (BECKMAN COULTER, USA), and the morphology of polymeric micelles and nanocomplexes were observed via transmission electron microscopy

(TEM).

### Stability measurements of nanocomplex

Nanocomplex (PMLA-PEI-DOX-TAT@PEG-DMMA) (0.5 mL, 1.0 mg/mL) was incubated with phosphate-buffered saline (PBS) (pH 7.4, 0.5 mL), or Roswell Park Memorial Institute (RPMI) 1640 medium contained 10% FBS (0.5 mL). At designated time intervals, the solution of nanocomplex was used for DLS measurements.

### Zeta potential analysis

The zeta potentials of nanocomplexes (PMLA-PEI-DOX-TAT@PEG-DMMA and PMLA-PEI-DOX-TAT@PEG-SA) were measured by photon correlation spectroscopy using Delsa™ Nano C Particle Analyzer (BECKMAN COULTER, USA) at 25 °C. Briefly, 2 mg of nanocomplexes was added into 2 mL PBS solution (phosphate buffered saline, pH 7.4 or pH 6.8). At designated time intervals, a certain volume of solution was withdrawn and used for zeta potential measurements.

### pH-responsive behaviors and in vitro DOX release

DOX-CA was incubated with different pH values of phosphate-buffered saline (PBS) solution (pH 4.0, pH 5.0, pH 6.8 and pH 7.4). At designated time intervals, the solution was used for high performance liquid chromatography (HPLC) (Shimadzu 1630, Japan) measurements. HPLC analysis was performed on Agilent 1260 Infinity LC system (Agilent, Germany). Chromatographic separation was carried out at room temperature on a CAPCELL PAK C18 column (3.0 mm × 100 mm, 3 μm, SHISEIDO, Japan). The mobile phase consisted of solvent A (sodium dodecyl sulfate solution), solvent B (acetonitrile) and solvent C (methanol). The flow rate was 0.8 ml/min and the injection volume was 10 μL. The detection wavelength was set to 254 nm. Then, the release rate of DOX from the nanocomplex (PMLA-PEI-DOX-TAT@PEG-DMMA) was investigated by a dialysis method. Typically, 1 mL of nanocomplex solution (2 mg/mL) was dialyzed (MWCO: 3.5 kDa) against 20 mL PBS solution (pH 7.4, 6.8 or 5.0) at 37 °C. At given intervals, 100 μL of external buffer was collected and replaced by the same volume PBS solution. The concentration of DOX released from polymeric micelles was quantified by ultraviolet spectrophotometry (Shimadzu, Japan) at 481 nm.

### Cell lines and culture

The human lung epithelial tumor cell line A549 and human hepatocellular carcinoma cell line MHCC97-H were obtained from the Cell Bank of Type Culture Collection of the Chinese Academy of Sciences. In all experiments, A549 cells and MHCC97-H cells were cultivated in RPMI-1640 and DMEM medium supplemented with 10% fetal bovine serum respectively at 37 °C in a humidified 5% CO2/95% air atmosphere.

### Flow cytometry

A549 cells and MHCC97-H cells were seeded into 6-well plates at a density of $3\times10^5$ cells/well and incubated overnight. For cellular internalization observation, cells were incubated with the polymeric micelles (PMLA-PEI-DOX and PMLA-PEI-DOX-TAT) or nanocomplexes (PMLA-PEI-DOX-TAT@PEG-SA and PMLA-PEI-DOX-TAT@PEG-DMMA) at an equivalent Cy3 concentration of 0.25 μg/mL of fresh culture medium at pH 7.4 or 6.8, respectively. After incubation for 4 h, the cells were washed three times with PBS solution. The cells were then harvested by trypsinization and centrifuged at 1000 rpm for 5 min, resuspended with 500 μL PBS and analyzed by a FACScan instrument (Becton Dickinson, USA).

### Confocal microscopy studies

Confocal fluorescent microscopy was used to compare the cellular uptake of Cy3 labeled polymeric micelles or nanocomplexes. Similar to flow cytometry, A549 cells and MHCC97-H cells were seeded into glass-bottomed dishes at a density of $3\times10^5$ cells/well and incubated overnight. Then, the cells were treated with various Cy3 labeled polymeric micelles or nanocomplexes in fresh culture medium at pH 7.4 or 6.8, respectively. After 4 h incubation, the cells were washed three times with PBS solution to remove the remnant growth medium and fixed in 4% paraformaldehyde for 10 min, followed by cell nuclei staining with DAPI for 15 min. After the cells were washed with PBS solution, fluorescent images of cells were analyzed by using a FV1000 confocal microscope (Olympus, Japan).

### In vitro cytotoxicity

The cytotoxicity of free DOX, polymeric micelles and nanocomplexes against A549 cells and MHCC97-H cells were investigated by using Cell Counting Kit-8 (CCK-8) assay. The cells were seeded into 96-well plates at a density of $1\times10^4$ cells per well and incubated overnight. Then the medium was replaced by free DOX, polymeric micelles or nanocomplexes in cell culture medium with different pH (6.8 or 7.4) and incubated for 48 h. After that, 10 μL CCK-8 solution was added to each well of the plate. Then, the plate was incubated for 2 h. Cell viability was determined by scanning with a microplate reader at 450 nm. The viability rate (VR)

was calculated according to the manufacturer's instructions. Besides, the cytotoxicity assessment of polymers (PMLA-PEI, PMLA-PEI-TAT, PEG-DMMA and PEG-SA) without DOX conjugated was also conducted similarly to the above process, at pH 7.4 with various concentrations (0.1 to 1000 μg/mL).

### Animals

Five-week-old BALB/c athymic nude mice (~ 20 g) were purchased from Peking University Health Science Center and feed at the condition of 25 °C and 55% of humidity. All animal experiments were approved by the Animal Research Committee of the Fourth Military Medical University and conducted in accordance with the international standards on animal welfare.

### In Vivo Tumor growth Inhibition Study

First, the tumors were built up by subcutaneous injection of A549 cells into the left axilla of each female mouse with a density of $5 \times 10^6$ cells in 100 μL PBS. After growing for 1 week, the tumors reached the size of about 6−8 mm. Then, the tumor-bearing mice were randomly divided into five groups (n = 4 for each group) and were treated by intravenous injection with saline, free DOX, PMLA-PEI-DOX-TAT, PMLA-PEI-DOX-TAT@PEG-SA and PMLA-PEI-DOX-TAT@PEG-DMMA, respectively. The injected amount for different polymeric micelle or nanocomplexes was 200 μL saline with DOX dose of 5 mg/kg body weight, and administered every 3 days. The tumor size and body weights were measured every day after the treatment.

### Biodistribution *in vivo*

The *in vivo* imaging system was used to study the biodistribution of Cy3-labeled polymeric micelle (PMLA-PEI-DOX-TAT) or nanocomplexes (PMLA-PEI-DOX-TAT@PEG-SA and PMLA-PEI-DOX-TAT@PEG-DMMA) in the A549 cell subcutaneous xenograft model in BALB/c athymic nude mice. The mice were observed at the 24 h after intravenous injection Cy3-labeled polymeric micelle or nanocomplexes at Cy3 dose of 0.1 mg/kg into the tumor-bearing mice.

### Histology and *in situ* cell death detection

Histology analysis was carried out at the 22$^{nt}$ day after the treatment. Typical heart, liver, spleen, lung, and kidney tissues of the mice in the control group and the best treatment group were isolated. Then, the organs were dehydrated using buffered formalin, ethanol with different concentrations, and xylene. After that, they were embedded in liquid paraffin. The sliced organs (3−5 mm) were stained with hematoxylin and eosin (H&E), and examined on a Leica SP8 microscope. In addition, Paraffin-embedded 5 μm thick tumor sections were obtained for the terminal transferase dUTP nick-end labeling (TUNEL) assay.

### Statistical analysis

The mean values ± SD were determined for all the treatment groups. Each value is the mean of at least three repetitive experiments in each group. Statistical analysis was performed by Student's t-test. The differences between two groups was considered significant for $*p<0.05$, and very significant for $**p<0.01$, $***p<0.001$.

## Abbreviation

PMLA: poly(β-L-malic acid); RES: reticuloendothelial system; NDDS: nanoscale drug delivery systems; EPR effect: enhanced permeation and retention effect; DMMA: 2,3-dimethylmaleic anhydride; SA: succinic anhydride; CA: *cis*-aconitic anhydride. TAT peptide: transactivator of transcription peptide; CPPs: cell-penetrating peptides; NMR: nuclear magnetic resonance; CMC: critical micelle concentration; HPLC: high performance liquid chromatography.

## Supplementary Material

Supplementary figures and tables.
http://www.thno.org/v07p1806s1.pdf

## Acknowledgements

The authors would like to acknowledge support from the National Natural Science Foundation of China (Grant No. 81271687 and 81571786).

## Competing Interests

The authors have declared that no competing interest exists.

## References

1. Siegel RL, Miller KD, Jemal A. Cancer statistics, 2016. CA: a cancer journal for clinicians. 2016;66:7-30.
2. Campagna M-C. Chemotherapy Complications. Hospital Medicine Clinics. 2016;5:400-12.
3. Coates A, Abraham S, Kaye SB, Sowerbutts T, Frewin C, Fox RM, et al. On the receiving end--patient perception of the side-effects of cancer chemotherapy. European journal of cancer & clinical oncology. 1983;19:203-8.
4. Peer D, Karp JM, Hong S, Farokhzad OC, Margalit R, Langer R. Nanocarriers as an emerging platform for cancer therapy. Nat Nano. 2007;2:751-60.
5. Misra R, Acharya S, Sahoo SK. Cancer nanotechnology: application of nanotechnology in cancer therapy. Drug Discovery Today. 2010;15:842-50.
6. Tiwari M. Nano cancer therapy strategies. Journal of Cancer Research and Therapeutics. 2012;8:19-22.
7. Greish K. Enhanced permeability and retention of macromolecular drugs in solid tumors: A royal gate for targeted anticancer nanomedicines. Journal of Drug Targeting. 2007;15:457-64.
8. Petros RA, DeSimone JM. Strategies in the design of nanoparticles for therapeutic applications. Nat Rev Drug Discov. 2010;9:615-27.
9. Barreto JA, O'Malley W, Kubeil M, Graham B, Stephan H, Spiccia L. Nanomaterials: applications in cancer imaging and therapy. Advanced materials. 2011;23:H18-40.

10. Wicki A, Witzigmann D, Balasubramanian V, Huwyler J. Nanomedicine in cancer therapy: Challenges, opportunities, and clinical applications. J Control Release. 2015;200:138-57.
11. Lim EK, Kim T, Paik S, Haam S, Huh YM, Lee K. Nanomaterials for Theranostics: Recent Advances and Future Challenges. Chem Rev. 2015;115:327-94.
12. Cheng R, Meng FH, Deng C, Zhong ZY. Bioresponsive polymeric nanotherapeutics for targeted cancer chemotherapy. Nano Today. 2015;10:656-70.
13. Huang ZW, Laurent V, Chetouani G, Ljubimova JY, Holler E, Benvegnu T, et al. New functional degradable and bio-compatible nanoparticles based on poly(malic acid) derivatives for site-specific anti-cancer drug delivery. International Journal of Pharmaceutics. 2012;423:84-92.
14. Lee B-S, Fujita M, Khazenzon NM, Wawrowsky KA, Wachsmann-Hogiu S, Farkas DL, et al. Polycefin, a New Prototype of a Multifunctional Nanoconjugate Based on Poly(β-l-malic acid) for Drug Delivery. Bioconjugate Chemistry. 2006;17:317-26.
15. Patil R, Ljubimov AV, Gangalum PR, Ding H, Portilla-Arias J, Wagner S, et al. MRI Virtual Biopsy and Treatment of Brain Metastatic Tumors with Targeted Nanobioconjugates: Nanoclinic in the Brain. ACS Nano. 2015;9:5594-608.
16. Ljubimova JY, Portilla-Arias J, Patil R, Ding H, Inoue S, Markman JL, et al. Toxicity and efficacy evaluation of multiple targeted polymalic acid conjugates for triple-negative breast cancer treatment. Journal of Drug Targeting. 2013;21:956-67.
17. Inoue S, Ding H, Portilla-Arias J, Hu J, Konda B, Fujita M, et al. Polymalic Acid–Based Nanobiopolymer Provides Efficient Systemic Breast Cancer Treatment by Inhibiting both HER2/neu Receptor Synthesis and Activity. Cancer Research. 2011;71:1454-64.
18. Zhou Q, Yang T, Qiao Y, Guo S, Zhu L, Wu H. Preparation of poly(β-L-malic acid)-based charge-conversional nanoconjugates for tumor-specific uptake and cellular delivery. International Journal of Nanomedicine. 2015;10:1941-52.
19. Lankveld DPK, Rayavarapu RG, Krystek P, Oomen AG, Verharen HW, van Leeuwen TG, et al. Blood clearance and tissue distribution of PEGylated and non-PEGylated gold nanorods after intravenous administration in rats. Nanomedicine. 2011;6:339-49.
20. Owens DE, 3rd, Peppas NA. Opsonization, biodistribution, and pharmacokinetics of polymeric nanoparticles. Int J Pharm. 2006;307:93-102.
21. Gratton SE, Ropp PA, Pohlhaus PD, Luft JC, Madden VJ, Napier ME, et al. The effect of particle design on cellular internalization pathways. Proceedings of the National Academy of Sciences of the United States of America. 2008;105:11613-8.
22. Knop K, Hoogenboom R, Fischer D, Schubert US. Poly(ethylene glycol) in Drug Delivery: Pros and Cons as Well as Potential Alternatives. Angew Chem Int Edit. 2010;49:6288-308.
23. Mintzer MA, Simanek EE. Nonviral vectors for gene delivery. Chem Rev. 2009;109:259-302.
24. Aoshima Y, Hokama R, Sou K, Sarker SR, Iida K, Nakamura H, et al. Cationic amino acid based lipids as effective nonviral gene delivery vectors for primary cultured neurons. ACS chemical neuroscience. 2013;4:1514-9.
25. Fischer D, Li Y, Ahlemeyer B, Krieglstein J, Kissel T. In vitro cytotoxicity testing of polycations: influence of polymer structure on cell viability and hemolysis. Biomaterials. 2003;24:1121-31.
26. Ma SF, Nishikawa M, Katsumi H, Yamashita F, Hashida M. Cationic charge-dependent hepatic delivery of amidated serum albumin. J Control Release. 2005;102:583-94.
27. Jin E, Zhang B, Sun X, Zhou Z, Ma X, Sun Q, et al. Acid-Active Cell-Penetrating Peptides for in Vivo Tumor-Targeted Drug Delivery. Journal of the American Chemical Society. 2013;135:933-40.
28. Vives E, Richard JP, Rispal C, Lebleu B. TAT Peptide Internalization: Seeking the Mechanism of Entry. Current Protein & Peptide Science. 2003;4:125-32.
29. Heiden MGV, Cantley LC, Thompson CB. Understanding the Warburg Effect: The Metabolic Requirements of Cell Proliferation. Science. 2009;324:1029-33.
30. Helmlinger G, Sckell A, Dellian M, Forbes NS, Jain RK. Acid Production in Glycolysis-impaired Tumors Provides New Insights into Tumor Metabolism. Clinical Cancer Research. 2002;8:1284-91.
31. Du JZ, Sun TM, Song WJ, Wu J, Wang J. A Tumor-Acidity-Activated Charge-Conversional Nanogel as an Intelligent Vehicle for Promoted Tumoral-Cell Uptake and Drug Delivery. Angew Chem Int Edit. 2010;49:3621-6.
32. Li L, Yang QQ, Zhou Z, Zhong JJ, Huang Y. Doxorubicin-loaded, charge reversible, folate modified HPMA copolymer conjugates for active cancer cell targeting. Biomaterials. 2014;35:5171-87.
33. Yuan YY, Mao CQ, Du XJ, Du JZ, Wang F, Wang J. Surface Charge Switchable Nanoparticles Based on Zwitterionic Polymer for Enhanced Drug Delivery to Tumor. Advanced materials. 2012;24:5476-80.
34. Kirby AJ, Lancaster PW. Structure and efficiency in intramolecular and enzymic catalysis. Catalysis of amide hydrolysis by the carboxy-group of substituted maleamic acids. Journal of the Chemical Society, Perkin Transactions 2. 1972:1206-14.
35. Kirby AJ, McDonald RS, Smith CR. Intramolecular catalysis of amide hydrolysis by two carboxy-groups. Journal of the Chemical Society, Perkin Transactions 2. 1974:1495-504.